Experimental and computer conversion values are tabulated in Table 1 and Figure 6 presents typical calculations of conversion up the column for the first four experiments with 10% water and 3.8-9.9% catalyst. The figure shows how conversion is increased with increasing catalyst concentration and column height. Due to sampling difficulties it was not possible to measure the conversion along the column, except at the top, i.e., after phase separation was complete. The experimental conversion values at the top of the column are given in Figure 6 and good agreement was achieved between experimental and calculated conversion values.

NOTATION

A = water
a = interfacial area per unit volume
B = acetic acid
C = n-Butyl alcohol
D = n-Heptane
E = n-Butyl acetate
H = total height of column
h = height from bottom of column
K_G = overall mass transfer coefficient
k_2 = second order forward reaction rate constant
k_2' = second order reverse reaction rate constant
L = light phase flow
O/W = oil in water
S = cross-sectional area of column
S' = sulphuric acid
U = fluid velocity
V = heavy phase flow
W/O = water in oil
X = mole fraction

Greek Letters

δ = density
ϕ = volumetric hold-up
ν = stoichiometric coefficient

Subscripts

A,B,C = components, $A,B,C, \ldots$, respectively
X_{AB} = mole fraction of A in B rich phase
c = continuous phase
H = top of column
o = bottom of column

LITERATURE CITED

Al-Hemeri, A. A., "The Effect of Surface Renewal on Mass Transfer in Agitated Contactors," Ph.D. Thesis, University of Aston in Birmingham (1973).

Chartres, R. H., and W. J. Korchinsky, "Drop Size and Extraction Efficiency Measurements in a Rotating Disc Contactor," *Trans. Inst. Chem. Eng.*, **56**, 91 (1978).

Davies, G. A., and G. V. Jeffreys, "Coalescence and Phase Separation," Chapter 14, *Recent Advances in Liquid-Liquid Extraction*, E. Hanson, Pergammon Press (1971).

Edwards, C. A., and D. Himmelblau, "Mass Transfer Between Liquid Phases," *Ind. Eng. Chem.*, **53**, 229 (1961).

Komasawa, I., and J. Ingham, "Effect of System Properties on the Performance of Liquid-Liquid Extraction Columns," *Chem. Eng. Sci.*, **33**, 341 (1978).

Kung, E. Y., and R. G. Beckmann, "Dispersed Phase Hold-ups in a Rotating Disc Extraction Column," *AIChE J.*, **7**, 319 (1961).

Laddha, G. S., T. E. Degaleesan and R. Kannappan, "Hydrodynamic and Mass Transport in Rotary Disc Contactors," *C. and J. Chem. Eng.*, **56**, 137 (1978).

Lawson, G. and G. V. Jeffreys, "Effect of Mass Transfer on the Rate of Coalescence of Single Drops at a Plane Interface," *Trans. Inst. Che. Eng.*, **43**, 294 (1965).

Lewis, J. B., "The Mechanism of Mass Transfer of Solutes Across Liquid-Liquid Interfacies," *Chem. Eng. Sci.*, **8**, 295 (1958).

Mumford, C. J., and A. A. Al-Hemeri, "Effect of Surface Renewal and Mass Transfer in Agitated Columns," *Proc. ISEC*, Lyon, **2**, 1591 (1974).

Robinson, J. D., and S. Hartland, "Effect of Adjacent Drops on the Shape of a Drop Approaching a Liquid Interface," *Proc. ISEC*, **1**, 418 (1971).

Sarkar, S., "Liquid-Liquid Extraction with Chemical Reaction in Agitated Columns," Ph.D. Thesis, University of Aston in Birmingham (1976).

Manuscript received April 18, 1979; revision received and accepted October 24, 1980.

An Analytical Carnahan-Starling-van der Waals Model for Solubility of Hydrocarbon Solids in Supercritical Fluids

K. P. JOHNSTON

and

C. A. ECKERT

Department of Chemical Engineering
University of Illinois, Urbana, IL 61801

Data have been taken by a new flow technique for the solubility of nonpolar hydrocarbons in nonpolar supercritical fluids. These results for molecularly simple molecules provide a basis for the analytical representation of such systems by relatively simple equations of state.

SCOPE

Supercritical fluid extraction (SFE) is a new separation process which can offer substantial advantages in certain situations. Although many applications of SFE have appeared in the patent literature, there is no fundamental understanding of the phase behavior. For rational process design it would be highly desirable to have appropriate mathematical models of the thermodynamic behavior of supercritical solutions. The first purpose of this work was to establish a data base of molecularly simple supercritical solubility data. In order to gain the advan-

tages of working near infinite dilution, systems with relatively low solubilities were chosen. For ease of data interpretation, solid solutes were chosen. A second goal was to apply as simple a theoretical model as possible to represent the data.

Actually, these data would represent two regimes: the near supercritical where pressures and solubilities are relatively low and the solvent compressibility is quite high, and the denser supercritical region where pressures and solubilities are higher and the fluid is relatively incompressible. The former of these is the more difficult to model as nearly all analytical equations of state are poorest in the near supercritical region. The second is probably of more practical interest as it represents the region in which industrial SFE appears most feasible. Thus to be most useful the analysis should represent the dense supercritical region well.

CONCLUSIONS AND SIGNIFICANCE

A dynamic experimental technique was used to gather data on the solubilities of naphthalene, anthracene, and phenanthrene in supercritical ethylene at temperatures just above the critical temperature of the solvent and pressures up to 400 atm (1 atm = 1.01325 bar). The solubility correlates best with density as an independent variable and is in fact linear on a plot of log solubility versus solvent density. Such behavior is predicted by van der Waals type equations, and a Carnahan-Starling-van der Waals approach represents the data quite well with a minimum of adjustable parameters in the dense supercritical region. It has the advantage of not requiring critical point data for the solute, and the unlike pair interaction term a_{12} correlates with the enthalpy of vaporization of the solute. These results form a basis for the interpretation and correlation of phase equilibrium data for industrial SFE.

INTRODUCTION

Heavy nonvolatile organic molecules dissolve in supercritical fluids in excess of up to ten orders of magnitude above the ideal gas amount. These fluids, which often have "liquid-like" density, promote strong solvation, thus this solubility enhancement. A recent outbreak of proposals in the food, pharmaceutical, and petrochemical industries offer SFE as an alternative to liquid extraction. The present goal is to gain a fundamental qualitative and quantitative understanding of the SFE process, that will permit correlation and ultimately prediction of the thermodynamic behavior.

Since the fluid is highly compressible in the near supercritical region, the strong solvation forces cause the mixture to contract with very large negative values of the partial molar volume of the solute. The theoretical quantification of this effect is sufficiently complex that its success demands an interplay with experiments on the simplest possible molecules. The solubilities were measured for solid nonpolar hydrocarbon solutes in ethylene, at levels sufficiently low to approach infinite dilution. Unlike the situation with liquid solutes, the fluid does not dissolve into the solid solute phase. A simple van der Waals picture can describe the nonpolar forces in the dense supercritical region, and the solute-solute forces can be avoided at infinite dilution.

A unique property of this process is that the dissolved extract and solvent may be separated, thoroughly and reversibly, by decreasing the fluid density, thus its dissolving power. This may be accomplished by expansion to subcritical pressure, or by a relatively small increase in temperature. Compared to conventional distillation of non-volatile molecules, the new process often allows for significant energy savings, for example, in the de-asphalting of petroleum residuum (Gearhart and Garwin, 1976). It also allows for the separation of thermally labile substances. The problem of residual solvent entrainment of toxic organic solvents, often encountered in liquid extraction, is eliminated. Additional flexibility in selectivity for a series of extracts may be achieved through controlling pressure, temperature, and choice of solvent (Zosel, 1978; Gangoli and Thodos, 1977).

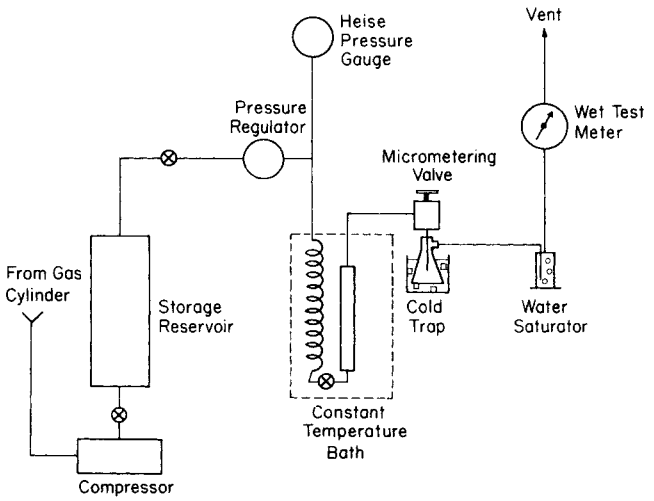

Figure 1. Schematic of flow apparatus for measuring solute solubility in supercritical fluids.

DYNAMIC EXPERIMENT FOR MEASUREMENT OF SOLID-FLUID EQUILIBRIA

A new flow apparatus was designed which offered several advantages over the conventional static methods of Diepen and Scheffer (1948), (1953) and Tsekhanskaya et al. (1965). The equilibration time was greatly reduced due to increased surface area of contact between the packed solid and flowing gas; furthermore, the solution was separated completely by depressurization to one atmosphere thus simplifying sampling and composition analysis (see Figure 1). A solid solute was packed into the 15 cm by 0.79 cm ID column or saturator in the constant temperature bath. The solvent gas was compressed into the reservoir and bled into the system at a regulated pressure (spring-loaded regulator), and at a flow rate controlled by a 0.157 cm orifice micrometering valve. The solvent reached bath temperature in an immersed heat exchange coil and then equilibrated with the solute. Next, the fluid was flashed to ambient pressure and the solute collected in a cold trap. Finally, the volume of gas flow was measured with a calibrated wet test meter.

The solubility was found from the weight gain in the trap, coupled with known temperature (±0.05°C), pressure (±0.3 bar) and gas flow. A sufficient amount of solid was initially collected in a waste trap until the saturator equilibrated with respect to composition, temperature, and pressure, then a tared trap was substituted. A run was completed by removing the trap

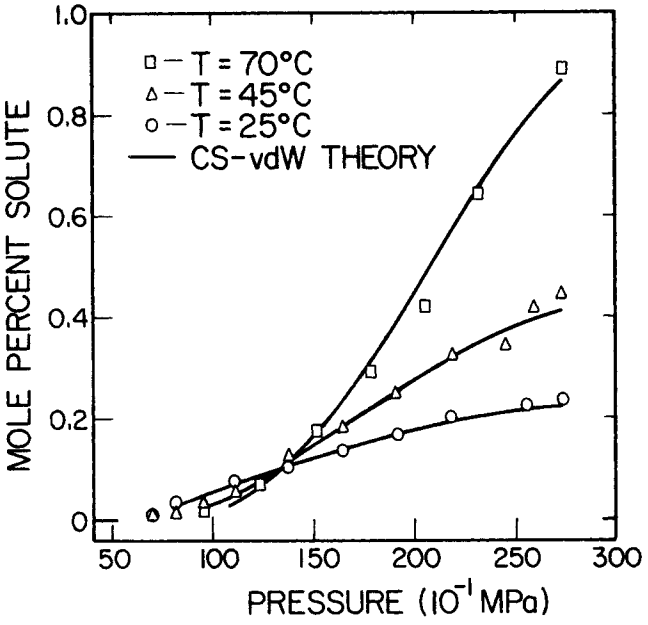

Figure 2. Comparison of predictions of the CS-VDW model with experimental data for the solubility of phenanthrene in ethylene.

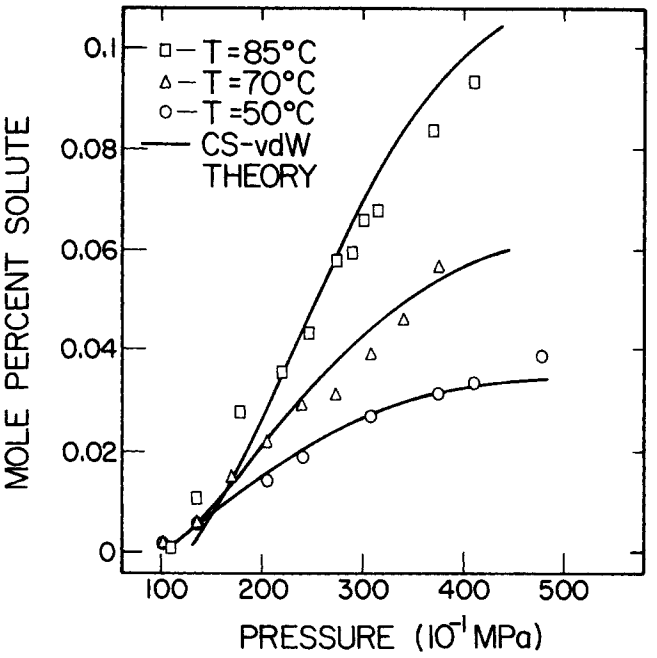

Figure 3. Comparison of predictions of the CS-VDW model with experimental data for the solubility of anthracene in ethylene.

TABLE 1. SOLUBILITY DATA FOR NAPHTHALENE, PHENANTHRENE AND ANTHRACENE IN ETHYLENE

Naphthalene		Phenanthrene		Anthracene	
Pressure 10^{-1} MPa	$y_2 \times 100$	Pressure 10^{-1} MPa	$y_2 \times 100$	Pressure 10^{-1} MPa	$y_2 \times 100$
25°C		25°C		50°C	
56.1	0.031	56.1	0.00137	138.8	0.00599
76.8	0.491	69.9	0.00905	207.8	0.0144
83.7	0.681	76.8	0.0193	242.3	0.0189
90.6	0.782	83.7	0.0314	311.3	0.0270
97.4	0.899	111.3	0.0722	380.2	0.0308
104.4	1.06	138.8	0.102	414.6	0.0336
118.2	1.16	166.5	0.131	483.6	0.0392
125.0	1.32	194.0	0.165		
138.8	1.48	221.6	0.200	70°C	
173.4	1.89	249.2	0.224		
		276.7	0.237	104.4	0.00172
45°C				138.8	0.00686
		45°C		173.4	0.0148
83.7	0.398			207.8	0.0214
104.4	1.04	69.9	0.00363	242.3	0.0290
125.0	2.01	83.7	0.0101	276.7	0.0309
138.8	2.83	97.5	0.0306	311.3	0.0388
152.7	3.51	111.3	0.0573	345.7	0.0458
		138.8	0.120	380.2	0.0572
50°C		166.5	0.183		
		194.0	0.246	85°C	
83.7	0.257	221.6	0.320		
111.3	1.32	249.2	0.339	111.4	0.00734
138.8	3.14	263.0	0.415	138.9	0.00988
166.5	5.37	276.7	0.443	180.3	0.0278
				221.6	0.0358
		70°C		249.3	0.0436
				249.3	0.0449
		69.9	0.00531	276.8	0.0495
		97.5	0.0207	276.8	0.0581
		125.0	0.0714	290.6	0.0594
		152.7	0.173	304.4	0.0660
		180.3	0.292	318.2	0.0674
		207.8	0.418	373.3	0.0838
		235.4	0.642	414.7	0.0930
		276.7	0.890		

while the saturator remained at the experimental pressure to avoid venting solution at other pressures through the trap. The complication of precipitation in the valve was overcome by minimizing the tubing length between the saturator and valve, and by heating the valve to melt any solid.

The 2-5% uncertainty in solubility corresponded directly to the uncertainty in weight gain in the trap, whereas the contributions from uncertainties in temperature, pressure, and gas flow were usually negligible. The exception is within about 15°C of the solvent critical temperature and 30 bars of the critical pressure where $(\partial y_2/\partial P)_T$ is large and small pressure deviations may cause approximately 2% uncertainty in solubility. A more detailed explanation of the apparatus and procedure was given by Johnston (1979).

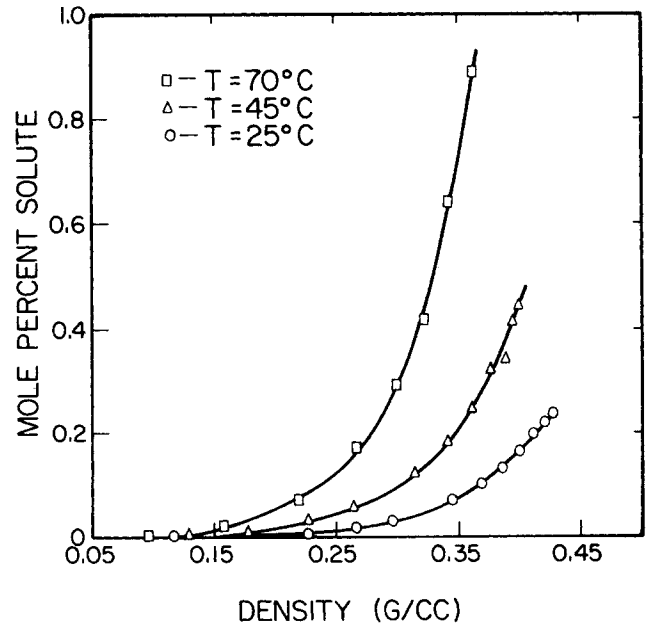

Figure 4. Solubility-density isotherms for phenanthrene in ethylene.

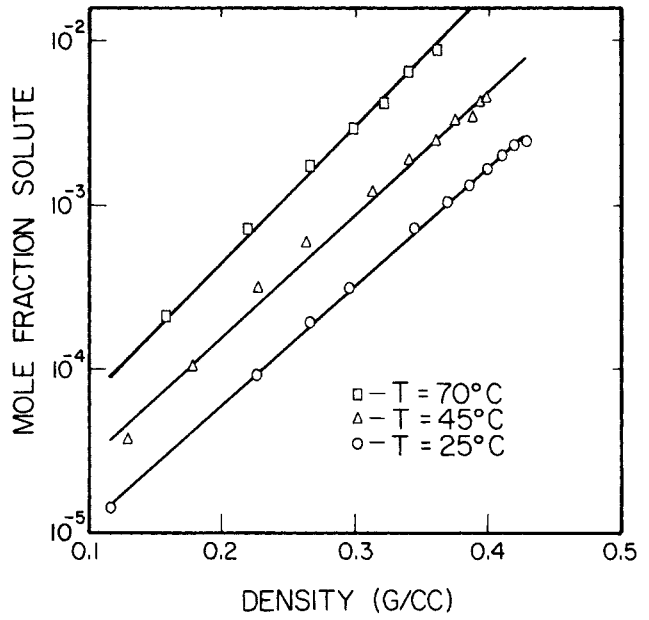

Figure 5. Solubility of phenanthrene in ethylene, log solubility versus density plot.

EXPERIMENTAL RESULTS

Three solubility versus pressure isotherms were measured for each of three binary systems: Naphthalene, phenanthrene, and anthracene in ethylene as shown in Figures 2 and 3 and Table 1. The results for naphthalene agreed with the data of Diepen and Scheffer (1948, 1953) and Tsekhanskaya et al. (1965) to within 2%. Furthermore, constant solubilities were measured for a five-fold range of flow rate thereby indicating that the saturator reached equilibrium.

The results suggest that the solute vapor pressure gives a good first approximation to the degree of solubility as shown by naphthalene > phenanthrene > anthracene. Note that at lower pressures the solubility is slightly higher at the lower temperatures, whereas at the higher pressures the solubility increases markedly with temperature. The former is due to the decrease in solvent density with increasing temperature, whereas the latter effect, in the dense, relatively incompressible region, is due primarily to the solid vapor pressure.

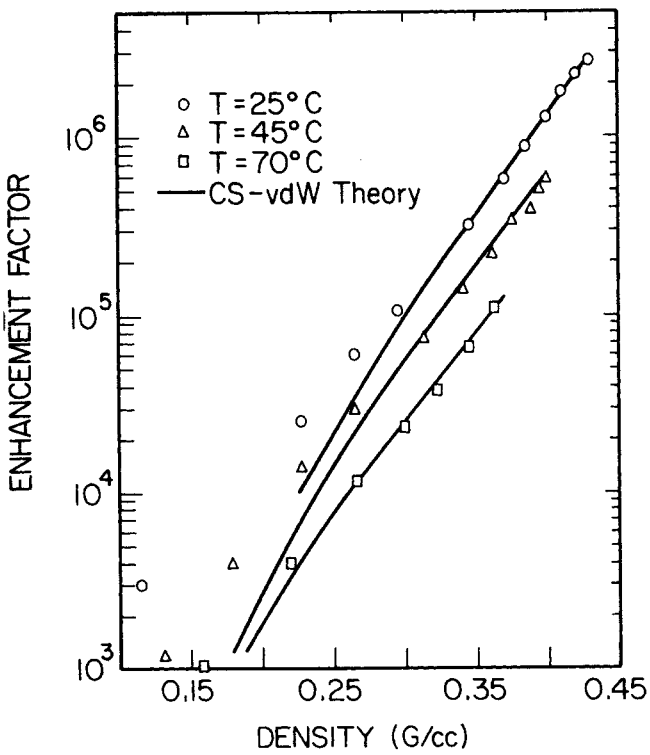

Figure 6. Linear experimental log enhancement factor versus density relationship predicted by VDW models only in the dense supercritical region.

A more meaningful representation of the data may be realized by removing the solvent density dependence on pressure (Figure 4). As the solvent density reaches a threshold level of approximately 0.25 g/cc for ethylene, the solubilities increase strongly with density, due to the existence of strong attractive forces between the solute and the surrounding molecules. In fact, the log of the solubility is fairly linearly related to solvent density as shown in Figure 5.

It is convenient to group the nonidealities in the fluid phase into an enhancement factor E, such that it describes the actual solubility normalized by the ideal solubility (P_2^{sat}/P)

$$E = \frac{y_2 P}{P_2^{sat}} \tag{1}$$

As shown in Figure 6, the value of E is roughly linear in density and corresponds to nonidealities of 10^3-10^6.

THEORETICAL APPROACH USING THE VAN DER WAALS MODEL

There are two separate questions regarding the success of these models. First, is the van der Waals (VDW) picture applicable, and if so, what is the most physically meaningful method to obtain the VDW parameters? Chandler (1978) describes the physics of the VDW picture, and Vera and Prausnitz (1972) derive six different equations of state by varying excluded volume and attractive force expressions used in the VDW partition function. All VDW methods represent data poorly in the near supercritical reduced density region of about 1-1.5. Furthermore, in the high density range, the differences between the various VDW equations of state are relatively immaterial in correlating the data.

The two alternatives for equating the chemical potential of the solid and fluid phases are to consider the fluid to be: (1) an "expanded" liquid or (2) a highly nonideal gas. In either case, the fugacity of the solid is:

$$f_2^S = f_2^{0S} \exp \frac{v_2(P - P_2^{sat})}{RT}. \tag{2}$$

The above two alternatives for the fluid phase yield:

$$f_2^L = f_2^{0L}(P^0)\gamma_2(P^0, x_2)x_2 \exp \int_{P^0}^{P} \frac{\bar{v}_2(x_2, P)dP}{RT} \tag{3}$$

$$f_2^V = \phi_2 y_2 P. \tag{4}$$

In the critical region, where the liquid and gas phases converge, it is thermodynamically sound to extrapolate the fugacity coefficient to the liquid phase, and the activity coefficient to the gaseous phase. Both methods require the integral of $\bar{v}_i dP$; however, partial molar volume data in the critical region are rare, and such data as a function of P and T are usually nonexistent.

SOLID-FLUID EQUILIBRIA MODEL USING CRITICAL PROPERTIES

Mackay and Paulaitis (1979) treated the fluid as an "expanded liquid" and then equated Eqs. 2 and 3. They used the Redlich-Kwong equation, along with the mixing rules of Chueh and Prausnitz (1967), to calculate $\bar{v}_2$. They used the critical pressure for the reference state, and assumed that γ_2 and $\bar{v}_2$ could be considered to be at infinite dilution. The pure-component fugacity ratio for the solid and subcooled liquid was explained without using vapor pressures. Although this correlation fit the data to within about 10%, the adjustable parameter γ_2^∞ was as high as 1500 which may not be physically meaningful. The other parameter, k_{12}, the deviation from the geometric mean temperature mixing rule, was somewhat different from the values given by Chueh and Prausnitz (1967).

A corresponding states theory for highly asymmetric systems based on the critical properties is problematic for several reasons:

TABLE 2. EQUATION OF STATE AND FUGACITY COEFFICIENT FOR SEVERAL VAN DER WAALS MODELS

	CS-VDW	RK	CS-RK
Equation of State	$P = RT\left(\frac{\xi}{b_o}\right)\frac{(1+\xi+\xi^2-\xi^3)}{(1-\xi)^3} - a/v^2$ (5)	$P = \frac{RT}{v-b} - \frac{a}{T^{1/2}v(v+b)}$ (6)	$P = RT\left(\frac{\xi}{b_o}\right)\frac{(1+\xi+\xi^2-\xi^3)}{(1-\xi)^3} - \frac{a}{T^{1/2}v(v+b)}$ (7)
Fugacity Coefficient (assuming $b \sim b^{\text{effective}}$)	$ln(\phi_2 Z) = \frac{3\xi^3-9\xi^2+8\xi}{(1-\xi)^3} - \frac{2(y_1a_{12}+y_2a_{22})}{RTv}$ (8)	$ln(\phi_2 Z) = ln\frac{v}{v-b} + \frac{b}{v-b} - \frac{2(y_1a_{12}+y_2a_{22})}{RT^{3/2}b} ln\frac{v+b}{v} + \frac{(y_1^2a_{11}+2y_1y_2a_{12})}{RT^{3/2}b}\left[ln\frac{v+b}{v} - \frac{b}{v+b}\right]$ (9)	$ln(\phi_2 Z) = \frac{3\xi^3-9\xi^2+8\xi}{(1-\xi)^3} - \frac{2(y_1a_{12}+y_2a_{22})}{RT^{3/2}b} ln\frac{v+b}{v} + \frac{(y_1^2a_{11}+2y_1y_2a_{12})}{RT^{3/2}b}\left[ln\frac{v+b}{v} - \frac{b}{v+b}\right]$ (10)

1. The vastly different critical properties of the large solute and small solvent undermine the validity of choosing a corresponding state that can possibly describe the molecular interactions of such different natures.
2. A mixing rule used to combine critical properties of pure fluids to a mixture critical property, when the original fluids have vastly different critical properties, is questionable. For example, a small molecule instantaneously interacts with only part of a large molecule.

SOLID-FLUID EQUILIBRIA MODEL WITHOUT USING CRITICAL PROPERTIES

A key improvement in the proposed model is avoidance of the need for solute critical properties, which are often unavailable. Even if available, their meaning in relation to pure *P-V-T* properties has not been experimentally verified. The proposed approach is formulated by analyzing the VDW picture of dense fluids, which for supercritical fluids is only useful for a reduced density above about 1.5. The harsh repulsive forces, which are nearly hard core interactions, dominate the structure of the liquid. The attractive forces affect structure only slightly, while strongly influencing the thermodynamic properties as a mean field that stabilizes this high density.

Consider the case of a solution at infinite dilution. The solute promotes strong attractive forces with the solvent that stabilize the dense fluid resulting in a solubility enhancement. In the high density region, this stabilization only weakly influences the structure as explained above, and the VDW attractive term is applicable. At infinite dilution, the solute does not significantly affect the excluded volume or repulsive forces of the mixture. This will not be the case in the near supercritical region, where the structure of the highly compressible fluid is subject to complex effects beyond the realm of VDW theory.

It is assumed that the effective repulsive parameter is strongly dependent on the excluded volume of the solvent, and rather invariant for a series of solutes. This assumption was tested with the Carnahan-Starling-van der Waals (CS-VDW), the Redlich-Kwong (RK), and the Carnahan-Starling-Redlich-Kwong (CS-RK) equations, which are all VDW models (Carnahan and Starling, 1972), Table 2. Carnahan and Starling (1972) found the three give similar results for pure fluids. Using a one fluid mixing rule:

$$a = y_1^2a_{11} + 2y_1y_2a_{12} + y_2^2a_{22} \tag{11}$$

and

$$b = y_1b_1 + y_2b_2 \approx b^{\text{effective}} \tag{12}$$

for each equation of state with the expression for the fugacity coefficient,

$$RT\ ln\ f_i/(y_iP) = \int_V^\infty \left[\left(\frac{\partial P}{\partial n_i}\right)_{T,V,nj} - \frac{RT}{V}\right]dV - RT\ ln\ Z \tag{13}$$

gives the results for $ln\ \phi_2$ shown in Table 2. Notice these models include a_{11} and b that may be determined for the pure solvent, and a_{12}, the only adjustable parameter dependent on the solute.

TABLE 3. REPULSIVE AND ATTRACTIVE PARAMETERS FOR THE CS-VDW EQUATION, OBTAINED FROM THE SOLUBILITY DATA

System	P 10^{-1} MPa	T (°C)	b (cm³/gmol)	$a_{12} \times 10^{-6}$ (MPa-cm⁶/gmol²)
Naphthalene-Ethylene	77-173	25	28	1.65
	84-153	45	28	1.70
	84-167	50	28	1.72
Phenanthrene-Ethylene	84-277	25	28	1.98
	111-277	45	28	1.95
	125-277	70	28	1.92
Anthracene-Ethylene	139-484	50	28	1.88
	139-380	70	28	1.86
	139-415	85	28	1.86
Naphthalene-CO_2	130-330	35	12.5	0.75
	125-310	45	12.5	0.76
(Data of Tsekhanskaya et al., 1965)	130-320	55	12.5	0.78

TABLE 4. COMPARISON OF THE THREE VDW MODELS, ALONG WITH THE RK MODEL USING CRITICAL PROPERTIES

(standard deviation/mean[1] in y_2 given in each case)

	T (°C)	Without Critical Properties CS-VDW	RK[2]	CS-RK[2]	RK[3] With Critical Properties	
Phenanthrene-Ethylene	25	0.065	0.074	0.051	0.091	(11.8)
	45	0.104	0.141	0.074	0.120	(11.2)
	70	0.098	0.089	0.146	0.224	(10.1)
Anthracene-Ethylene	50	0.129	0.124	0.071	0.317	(10.9)
	70	0.125	0.153	0.107	0.241	(10.5)
	85	0.101	0.190	0.075	0.188	(9.83)

1. standard deviation/mean $= \frac{\left[\sum_{i=1}^{n}(y_{2i}^{\text{exp}} - y_{2i}^{\text{calc}})^2\right]^{1/2}}{(n-1)^{1/2}\bar{y}_2^{\text{exp}}}$
2. $a_{11} = 7.953 \times 10^6$ MPa-cm⁶/gmol².
3. In both cases, optimized $k_{12} = 0.03$. The optimized value of $ln\gamma_2^\infty$ for each temperature is shown in parenthesis.

The solute attractive parameter a_{22}, may be neglected for low solubilities.

RESULTS OF CORRELATION FOR SOLID-FLUID EQUILIBRIA DATA

An expression for the solubility is obtained using Eqs. 2 and 4, with the fugacity coefficient described by one of Eqs. 8-10.

$$y_2 = \frac{P_2^{sat}\phi_2^{sat} \exp \frac{v_2(P - P_2^{sat})}{RT}}{\phi_2 P} \tag{14}$$

Notice ϕ_2^{sat} is unity for nonvolatile solids. In the range of infinite dilution, the solution density approaches the pure solvent density, thus the experimental densities of Din (1962) were used instead of using the equations of state 5-7. This circumvents the need for a_{11} in the CS-VDW expression, while it was obtained using critical properties in the other two VDW equations. The attractive parameter a_{12} was optimized using linear least squares for each choice of b, until the optimal value of b was found. Since a_{12} is related to the log of y_2 the experimental uncertainty in y_2 usually corresponded to an order of magnitude less uncertainty in a_{12}.

The results shown in Figures 2 and 3, and in Tables 3 and 4 suggest a reasonable correlation except in the near supercritical region where the attractive forces are complex and nonuniform. The consistency of the hard sphere parameter helps substantiate the assumption that it is invariant for a series of solutes. Notice the value of the effective b is greater than the b obtained for pure ethylene, about 20 cm^3/gmol. This effective hard sphere parameter includes contributions from the solute, without requiring a solute excluded volume that may be difficult to predict. The value of the effective b may be determined for the more suitable fluids such as ethylene, ethane, and carbon dioxide, in which it is expected to be nearly constant for a series of solutes.

The attractive parameter varied slightly with temperature, which would not be the case for the van der Waal's assumption that the radial distribution function is independent of temperature. Beret and Prausnitz (1975) demonstrated the effect of temperature and density on the attractive parameter for a pure square well fluid, based on molecular dynamics results. The attractive parameter increased or decreased with temperature depending upon the reduced density, in the same density range as the present solubility experiments. Oellrich et al. (1978) applied a second order polynomial to fit the temperature dependence of both the attractive and repulsive parameters for a variety of pure fluids.

The application of these methods to describe the slight temperature dependence of a_{12} for a mixture, thus the addition of many more adjustable parameters, is not worthwhile. Furthermore, this temperature effect could also be partially attributed to uncertainties in the vapor pressure data. Mackay and Paulaitis (1979) avoided the need for vapor pressure data; furthermore, the value of k_{12} was independent of temperature. The temperature dependence was advantageously incorporated into the activity coefficient, but the small deviation from linearity for the recommended fit of $ln\ \gamma_2^{\infty}$ vs. $1/T$ corresponds to the same uncertainty as noted for the temperature effects in the present model.

The a_{12} tends to follow a similar trend found by Kaul and Prausnitz (1977) at lower pressures for ϵ_{12} in the virial equation. Second virial coefficients were predicted for gas mixtures containing simple fluids and heavy hydrocarbons by fitting the crucial parameter ϵ_{12}, which cross-correlated well with the enthalpy of vaporization of the solute. The crucial parameter for solid-fluid equilibria, the solute-solvent attractive parameter a_{12}, appears to follow the same trend for cross-correlation. Furthermore, the larger value of a_{12} for naphthalene in ethylene versus carbon dioxide is consistent with the ϵ_{12} results.

Since $a_{22} > a_{12}$, the theoretical prediction of the solubilities should be low if a_{22} is important (Eq. 8), especially in the range of high solubilities. For most of the systems, the solubility correlation was good at the higher solubilities; however, the predicted values were low as expected in the case of naphthalene when the solubilities reached 3 mol%.

The CS-VDW equation gives insight to the nearly linear enhancement factor relationship shown in Figure 6. Combining Eqs. 1, 14 and 8 yields:

$$ln\ E = \frac{v_2(P - P_2^{sat})}{RT} - \frac{3\xi^3 - 9\xi^2 + 8\xi}{(1 - \xi)^3} + \frac{2(y_1 a_{12} + y_2 a_{22})}{RT\ v} + ln\ Z \tag{15}$$

Notice the attractive term suggests this linear relationship. The first and last terms contribute only a small fraction to $ln\ E$. The repulsive term is fairly linear in density for the range of interest. For this reason, the CS-VDW equation is slightly preferable to the other VDW forms along with the fact it has a more reasonable semi-theoretical basis, and it does not require a_{11}.

This new approach gave results similar to previous methods without the need for solute critical properties. Only one binary parameter was needed, that may be related to the enthalpy of vaporization of the solute. Once the equilibrium behavior is understood quantitatively in the dense region, where VDW theory holds, the more difficult undertaking will be to characterize the behavior in the highly complex near critical region.

ACKNOWLEDGMENT

The authors gratefully acknowledge the financial support of the General Foods Corp. and the U.S. Environmental Protection Agency.

NOTATION

a = attraction parameter for VDW models
b = hard-sphere parameter for VDW models
E = enhancement factor (y_2P/P_2^{sat}) or actual solubility divided by ideal solubility
f = fugacity
k = binary interaction parameter for deviations in the geometric-mean temperature mixing rule used for a_{12}
v = molar volume
$\bar{v}$ = partial molar volume
x = liquid mole fraction
y = vapor mole fraction
Z = compressibility factor

Greek Letters

ξ = dimensionless density (b/v)
ϕ = fugacity coefficient
γ = activity coefficient
ϵ = intermolecular potential energy used for virial coefficients

Subscripts

1, 2, = components

Superscripts

O = reference state
OL = pure liquid
OS = pure solid
V = vapor
sat = saturation
∞ = infinite dilution

LITERATURE CITED

Beret, S. and J. M. Prausnitz, "Perturbed Hard-Chain Theory: An Equation of State for Fluids Containing Small or Large Molecules," *AIChE J.*, **21**, 1123-1132 (1975).

Carnahan, N. F. and K. E. Starling, "Intermolecular Repulsions and the Equation of State for Fluids," *AIChE J.*, **18**, 1184-1189 (1972).
Chandler, D., "Structures of Molecular Liquids," *Ann. Rev. Phys. Chem.*, **29**, 441-71 (1978).
Chueh, P. L. and J. M. Prausnitz, "Vapor-Liquid Equilibria at High Pressures. Vapor-Phase Fugacity Coefficients in Non-Polar and Quantum-Gas Mixtures," *Ind. and Eng. Chem. Fund.*, **6**, 492 (1967).
Diepen, G. A. and F. E. Scheffer, "The Solubility of Naphthalene in Supercritical Ethylene," *J. Amer. Chem. Soc.*, **70**, 4085-4090 (1948).
Diepen, G. A. and F. E. Scheffer, "The Solubility of Naphthalene in Supercritical Ethylene II," *J. Phys. Chem.*, **57**, 575-577 (1953).
Din, F., *Thermodynamic Function of Gases*, **2**, Butterworths, London (1962).
Gangoli, N. and G. Thodos, "Liquid Fuels and Chemical Feedstocks from Coal by Supercritical Gas Extraction," *Ind. Eng. Chem. Prod. Res. Dev.*, **16**, 208-216 (1977).
Gearhart, J. A., and L. Garwin, "A New Economical Approach to Residuum Processing," NPRA Annual Meeting, AM-76-36 (March 30, 1976).
Johnston, K. P., "High-Pressure Phase Equilibria: The Solubility of Non-Volatile Molecules in Supercritical Fluids," M.S. Thesis, University of Illinois, Urbana, IL (1979).
Kaul, B. K. and J. M. Prausnitz, "Second Virial Coefficients of Gas Mixtures Containing Simple Fluids and Heavy Hydrocarbons," *Ind. Eng. Chem. Fundam.*, **16**, 335-340 (1977).
Mackay, M. E. and M. E. Paulaitis, "Solid Solubilities of Heavy Hydrocarbons in Supercritical Solvents," *Ind. Eng. Chem. Fundam.*, **18**, 149-153 (1979).
Oellrich, L. R., H. Knapp, and J. M. Prausnitz, "A Simple Perturbed Hard-Sphere Equation of State Applicable to Subcritical and Supercritical Temperatures," *Fluid Phase Equilibria*, **2**, 163-171 (1978).
Tsekhanskaya, Y. V., M. B. Iomtev, and E. V. Mushkina, "Solubility of Naphthalene in Ethylene and Carbon Dioxide Under Pressure," *Russ. J. Phys. Chem.*, **38**, 1173-1176 (1965).
Vera, J. H. and J. M. Prausnitz, "Generalized van der Waals Theory for Dense Fluids," *Chem. Eng. J.*, **3**, 1-13 (1972).
Zosel, K., "Separation with Supercritical Gases: Practical Applications," *Ang. Chemie Int. Ed.*, **17**, 702-709 (1978).

Manuscript received June 12, 1980; revision received October 30, and accepted November 21, 1980.

Studies in the Synthesis of Control Structures for Chemical Processes

YAMAN ARKUN

and

GEORGE STEPHANOPOULOS

Department of Chemical Engineering and Materials Science
University of Minnesota
Minneapolis, MN 55455

Part V: Design of Steady-State Optimizing Control Structures for Integrated Chemical Plants

This paper addresses the question of how to design the steady-state optimizing control system for a large scale interconnected chemical plant. The integrated design approach is structured within the framework of the hierarchical control theory and is based on the concepts of constraint control, hierarchical decomposition and nonlinear mathematical programming. Theoretical developments lead to the generation of alternative operational policies of practical value. An imbedded branch and bound screening strategy is given to select the best policy, which will be implemented on-line by the optimizing plant controllers. The general design approach has the broad applicability to any interconnected large scale system, and its application is demonstrated on a gasoline polymerization plant.

SCOPE

Process control tasks for a chemical plant consist of certain *regulatory* (i.e., product quality control, safety, environmental regulations, material balance control, etc.) and *economic* (i.e., most profitable steady-state plant operation) objectives, which have to be satisfied in the presence of a wide variety of plant disturbances. Typical disturbances are: changing raw material properties, different product specifications, varying market demands, fluctuating prices of raw materials and energy and many other external changes (e.g., ambient conditions, temperature drifts, pressure and flowrate changes, etc.). Classification of control objectives into two such categories formulates the different activities involved during the design of the regulatory and optimizing control structures. For further details on control tasks, the reader is referred to Morari, Arkun and Stephanopoulos (1980a).

In the last decade, extensive research has been conducted on the synthesis of process control structures (Govind and Powers,

Mr. Arkun is presently with the Department of Chemical and Environmental Engineering, Rensselaer Polytechnic Institute, Troy, NY 12181.

Parts I, II, and III of this paper appeared in *AIChE J.*, **26**, 220-260 (1980), and Part IV was published in *AIChE J.*, **26**, 975 (1980).